Impacts of COVID-19 restrictions on regional and local air quality across selected West African cities

Olusegun G. Fawole [1, 2], Najib Yusuf [3], Lukman A. Sunmonu [1], Aderonke Obafaye [3], Dauda K. Audu [3], Loretta Onuorah [4], Christiana F. Olusegun [3], Abdoulaye Deme [5], Habib Senghor [6]

[1] Department of Physics and Engineering Physics, Obafemi Awolowo University, Ile-Ife, Osun State, Nigeria

[2] School of the Environment, Geography and Geosciences, University of Portsmouth, Portsmouth, UK

[3] Centre for Atmospheric Research (CAR), National Space Research and Development Agency, Kogi State University, Anyigba Campus, Nigeria.

[4] Department of Physicial and Geosciences, Godfrey Okoye University, Enugu, Nigeria

[5] UFR Sciences Appliquees et Technologie (SAT), Universite Gaston Berger, Saint-Louis, Senegal

[6] Senegalese National Agency of Civil Aviation and Meteorology (ANACIM), Dakar, Senegal

Corresponding author: Olusegun G. Fawole (gofawole@oauife.edu.ng)

Key Point

1. There was a significant decrease in the level of aerosols, SO_2 and NO_2 over the sub-region and epicenters during the periods of lockdown
2. During the same period, there was a slight increase in ozone and CO over the sub-region and most of the epicenters
3. There is a shift in the size distribution of prevailing aerosol cluster towards the coarse fractions.

Abstract

The emergence of COVID-19 brought panic and a sense of urgency causing governments to impose strict restrictions on human and vehicular movement. With anthropogenic emissions, especially traffic and industrial activities, said to be a significant contributor to ambient air pollution, this study assessed the impacts of the imposed restrictions on the atmospheric

concentrations and size distribution of atmospheric aerosols and gaseous pollutants over West African sub-region and seven major COVID-19 epicenters in the sub-region. Satellite retrievals and reanalysis datasets were used to study the impact of the restrictions on Aerosol Optical Depth (AOD) and atmospheric concentrations NO_2, SO_2, CO and O_3. These anomalies were computed for 2020 relative to 2017-2019 (the reference years). In 2020 relative to the reference years, there was a significant reduction of between 0.5±24.6 – 13.7±30.3% and 5.9±17.1% in area-averaged AOD levels at the epicenters and over the sub-region, respectively. The levels of NO_2 and SO_2 also reduced substantially at the epicenters, especially during the periods when the restrictions were highly enforced. However, the atmospheric levels of CO and ozone increased slightly in 2020 compared to the reference years. This study shows that "a one cap fits all" policy cannot reduced the level of air pollutants and that traffic and industrial processes are not the major sources of CO in major cities in the sub-region. Although not available, ground-based measurements would have given a clearer and better picture of the anomalies observed with the dataset used in this study which are on a coarser spatial resolution.

Plain Language Summary

The emergence of COVID-19 in December 2020 caused national and regional governments to introduce lockdown and restrict the movement of vehicles and human. There was also a significant reduction or total stoppage of industrial activities. This study, in the absence of reliable long-term ground-based measurement of ambient air pollutants, used observations from satellites and reanalysis datasets to investigate the level of air pollutants in the air-shed of seven (7) major COVID-19 epicenters in the West Africa sub-region and also over the entire sub-region during the periods of lockdown. The level of pollutants during the pandemic in 2020 was

compared against the mean of the three preceding years (2017-2019) to calculate the anomalies. The level of aerosol (AOD), SO_2 and NO_2 reduced significantly in 2020 compared to the reference years. However, the atmospheric levels of ozone and CO increased slightly in 2020 as against the reference years. The slight increase in CO levels could be attributed to local burning of domestic waste and biomass burning. There was a shift in the size distribution of atmospheric aerosols cluster towards the coarse fraction.

1 Introduction

In late December 2019, an acute respiratory diseases was discovered in a cluster of humans in the indoor Huanan seafood wholesale market in Wuhan, Hubei province, China (Li et al., 2020). Symptoms of the diseases include fever, fatigue, cough and acute dyspnea (Fu et al., 2020; Rodriguez-Morales et al., 2020; Spychalski et al., 2020). The disease, later linked to the family

of coronaviruses, was named COVID-19 by the World Health Organization (WHO). COVID-19 was declared a Public Health Emergency of International Concern (PHEIC) on 30 January 2020 and a pandemic on 11 March 2020 (Eurosurveillance Editorial Team, 2020; Ntoumi and Velavan, 2021; Schwartz and Graham, 2020). Movement of people, especially tourists, during the Chinese New Year celebration in December 2019 was partly responsible for the fast spread of the diseases within and outside China (Bogoch et al., 2020; Chen and Yu, 2020; Yu and Chen, 2020).

Despite its widespread in Europe and Asia prompting the restriction of movements (human and vehicular) and the imposition of local, national and regional lockdowns and border controls by government at various levels, the epidemic did not become prevalent in Africa until mid-March 2020. While Egypt recorded the first case of the virus on February 14, twenty-seven (27) other African countries recorded their first cases between March 13 and 20, 2020 about 30 days after Egypt recorded its first case of the virus on the continent. The first case of the diseases was recorded in the seven (7) West African countries covered in this study – Nigeria, Senegal, Burkina Faso, Ghana, Cote D'ivoire, Cameroon and Mali – between February 28 and March 26, 2020. On the African continent, with 54 countries, it took 90 days for the number of confirmed cases to reach 100 000 but just 19 days to double the number of confirmed cases and another 12 days to reach 300 000 (Wadvalla, 2020). As at October 12, 2021, the cumulative number of cases and fatalities on the continent has risen to 6,087,812 and 121,597, respectively (data accessed from https://covid19.who.int on October 12, 2021).

From the aforementioned, it is clear that the spread of the pandemic to Africa started much later than other parts of the globe. In addition, the rate of infection and fatality on the African continent is much lower than projections made by international bodies e.g. the World Health

Organization (WHO) and Melinda Gates of the Bills and Melinda Gate Foundation (Njenga et al., 2020). The lower incidences and fatalities of COVID-19 experienced in Africa has been attributed to a number of factors including younger population, fewer percentage of the population living with comorbidities and life expectancy (Lawal, 2021). The first official COVID-19 death in Africa was announced on March 8, 2020 in Egypt.

Despite the relatively low incidences and fatalities, to curb the spread and resulting deaths, the government in most African countries were forced to resort to national or regional lockdowns – school and offices closures, shut down of industries, border closure (local and international) and restricted human and vehicular movement – so as not to put the already strained and under-funded healthcare systems in most African countries under pressure which could result in increased fatality figures. The periods of the lockdown run for weeks and even months at a stretch in the many African countries and occurred at different times but with overlaps during the first and second wave of the pandemic in 2020. Some countries eased the restriction briefly but had to re-impose it after experiencing significant spikes in the number of incidences and fatalities. Table 1 gives a breakdown of the periods of restriction in the seven West African countries considered in this study.

In most developing economies around the world, especially in low- and middle-income countries (LMICs), air quality (AQ) is at its lowest ebb owing to the fact the rapid economic and population growth and industrialization efforts experienced in most cities in LMICs are not backed up with sustainable management of the environment. The source of air pollutants in most West African cities is a combination of anthropogenic and biogenic, with pollutants from anthropogenic sources being the most dominant in urban air-sheds (Dominutti et al., 2019; Liousse et al., 2014; Marticorena et al., 2010; Naidja et al., 2018). In the West African sub-

region, most emissions from biogenic sources, e.g. desert dust and biomass burning, are often seasonal (Bauer et al., 2019). Anthropogenic sources of emissions include industrial processes, traffic and traffic-related, power generation, construction works, road dust re-suspension (Fayiga et al., 2018; Hoesly et al., 2018). Human activities and traffic are ubiquitous and often times uncontrolled and un-monitored in most cities in the sub-region where more than 80 % of automobiles on the roads are second-hand used vehicles imported from Europe and the US.

Globally, the COVID-19 pandemic led to unprecedented restrictions of movements that brought about a drastic reduction of global and local travels due to borders closures, closure of schools and businesses, including outright stoppage or massive reduction of industrial activities. As a result of these restrictions, many countries observed clear blue skies for the very first time in decades. Several studies in different regions of the world - Srivastava et al. (2021) (India), Menut et al. (2020) (Western Europe), Filonchyk et al. (2021) (Poland), Stratoulias and Nuthammachot (2020) (Thailand), Fuwape et al. (2021) (Nigeria) and Archer et al. (2020) (USA), just to mention a few - have reported significant improvement in AQ during the various lockdown periods which lasted for months in some countries, especially in epicenters and neighbouring cities.

Using AQ and meteorological data from ground-based and satellite platforms, studies from several countries and regions of the world have reported varying degrees of reduction in air pollution and Air Quality Indices (AQI), especially in COVID-19 epicenters. Serious dearth of long term AQ data from ground-based stations has greatly impacted air quality studies in most Africa countries. As such, studies on long-term trends and variability of atmospheric pollutants in this region have resorted to the use of data from remote sensing (e.g. AERONET, (Boiyo et al., 2017; Fawole et al., 2016; Yusuf et al., 2021)), reanalysis (e.g. MERRA-2, (Diop et al., 2018;

Veselovskii et al., 2018)) and satellite platforms (e.g. OMI; (Lourens et al., 2012; Marais et al., 2012)).

The anomalies were estimated as the atmospheric concentrations of the pollutants in 2020 relative to the mean of the three preceding years (2017-2019), herein referred to as the "reference years". Using aerosol optical depth (AOD), Angstrom Exponent (AE) and single scattering albedo (SSA), the study investigates the anomalies in the loading, size distribution and optical properties of dominant aerosols during the pandemic. To the best of the authors' knowledge, this is the first study to attempt an assessment of the anomalies of gaseous pollutant and aerosol loading as well as size distribution in the sub-region during the pandemic. This study brings into context the possible impact of mitigation strategies and other government policies to improve air quality in the study regions. It also shows the possible limitations which could impede the use of satellite retrievals for AQ monitoring in the sub-region, especially for the analyses of daily mean AQ levels.

In this study, we assessed and quantified the perceived anomalies in the atmospheric concentrations of four gaseous pollutants (NO_2, SO_2, O_3 and CO) and loading of atmospheric aerosol in 2020 in relation to historical mean (2017-2019). The authors hypothesized that: (i) there is a significant reduction in gaseous air pollutants in the West Africa sub-region brought about by months of limited human activities and restrictions of human and vehicular movements due to the COVID-19 pandemic and (ii) there is a reduction in the loading of atmospheric aerosol and a shift in size distribution of aerosol towards coarser aerosol cluster. The study area covers seven (7) West African countries with higher COVID-19 incidences and fatalities during the first and second waves.

2 Material and methods

2.1 Study area

The study area covers the seven epicenters and lies between 0^o S – 22^o N and 16^o W – 12^o E. The seven (7) epicenters were selected because of the relatively high number of COVID incidences and fatalities, and level of compliance/effectiveness and length of restrictions and lockdown periods. Table 1 shows, among other information, the coordinates of the epicenter in the selected countries and periods of restrictions. See Figure 1 for a map of the sub-region and the seven epicenters.

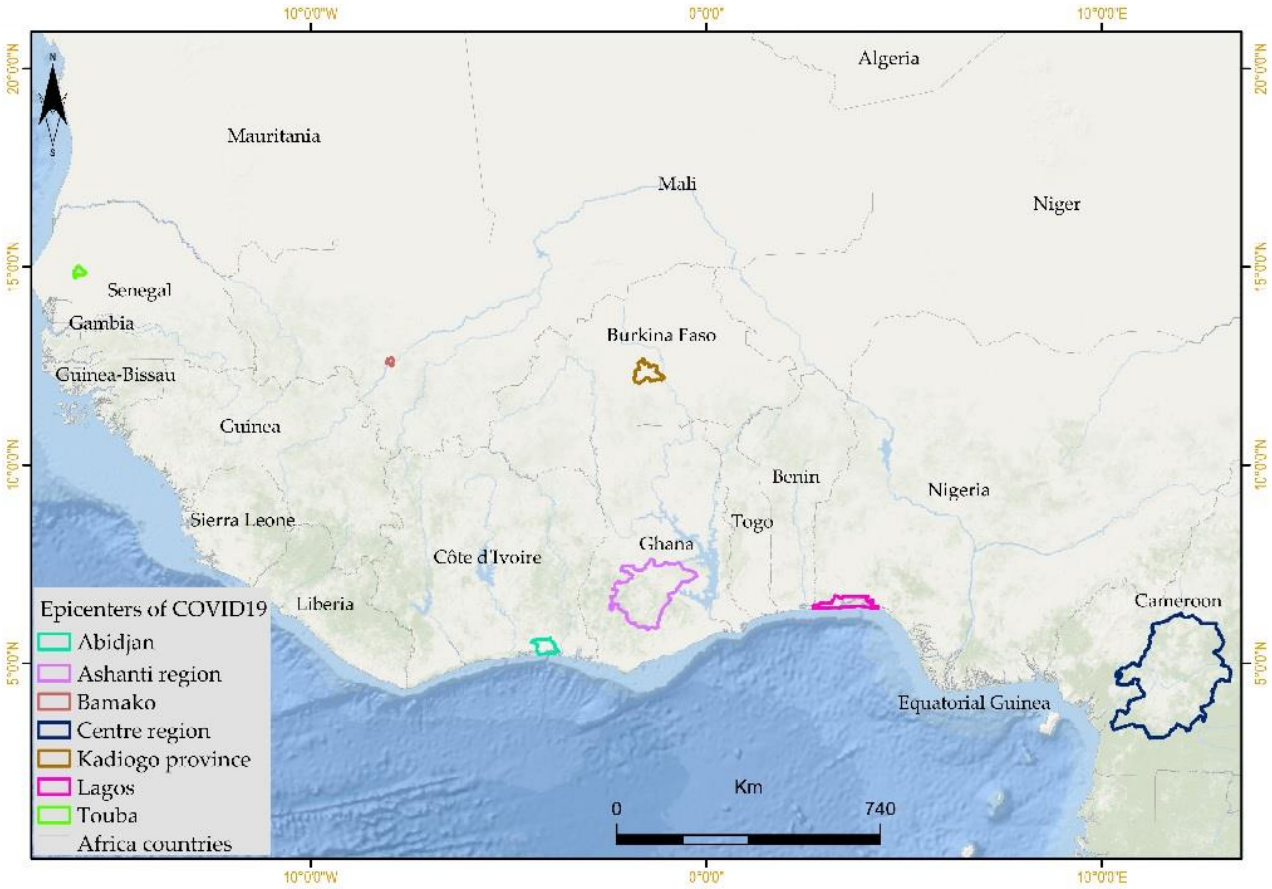

Figure 1: Map showing the sub-region and location of the seven (7) epicenters.

2.2 Government policies, lock-downs and restrictions

The seven (7) countries considered in this study implemented various closures and restrictions of movement at different periods during the 1st and 2nd waves of the pandemic between March and December 2020. The period of restrictions overlapped in most of the countries but the level of compliance varied. There were periods when the restrictions were relaxed in some part of the regions for a couple of days to a week before being re-imposed. Table 1 also gives a breakdown of the periods of restrictions and lock-downs including school and workplace closure, sit-at-home and border closure in the countries. Industrial activities were also totally halted or reduced to the very barest minimum. Only essential services were allowed to run unhindered during the period of restrictions. These restrictions brought almost a halt to human activities and traffic flow, especially in the epicenters where the restrictions on travels and workplaces were more effective and prolonged. As such, the comparisons intended in this study will be at the finer level of the epicenters in addition to the regional levels.

Table 1: Breakdown of the epicenters, locations and restriction periods in the study area

Country	Epicenter	Coordinate	Period of restrictions (approx.)*
Nigeria	Lagos	6.3 – 7^{o} N	March 30 – mid May
		2.7 – 4.3^{o} E	Mid July - September
Senegal	Touba	14.6 – 14.8^{o} N	March – June
		17.5 – 17.3^{o} W	August - October
Ghana	Accra & Ashanti Region	5.9 – 7.6 ^{o} N	March –July
		2.5 – 0.2^{o} W	Aug – September
Mali	Bamako	12.5 – 12.7^{o} N	March – May
		8.1 – 7.9 ^{o} W	July – September
Cote d'Ivoire	Abidjan	5.3 – 5.5 ^{o} N	March – June
		4.1 – 3.9 ^{o} W	August – September
Burkina Faso	Kadiogo Province	12 – 12.7 ^{o} N	March – April
		1.8 – 1.1 ^{o} W	August

Cameroun	Centre region	3.2 – 6.2 ^{o} N 10.2 – 13.2 ^{o} E	March – June July - August

* The periods of restrictions were estimated from https://graphics.reuters.com/world-coronavirus-tracker-and-maps/

2.3 Air Quality Data

The fact that reliable long-term ground-based air quality and meteorology data are not available in the study area is a well-known fact to the scientific community worldwide. As such, all the data acquired and processed for the intended analyses undertaken in this study are from satellite retrievals, model and remotely sensed data sources. All the data, aerosol and gaseous pollutant, were averaged to monthly values for ease of comparison of the various dataset included in the analyses.

Table 2: Source and specifications of pollutant used included in this study.

Pollutant	Source	Temporal resolution	Spatial resolution	Unit
SO_2 (surface mass concentration)	MERRA-2	Hourly	0.5 ^{o} x 0.625^{o}	kg/m^3
Ozone (total column)	OMI	Daily	0.25 ^{o} x 0.25 ^{o}	Dobson
CO (column burden)	MERRA-2	Monthly	0.5^{o} x 0.625^{o}	kg/m^2
NO_2 (total column) 30% cloud screened	OMI	Daily	0.25^{o} x 0.25^{o}	1/cm^2
Aerosol (AOD) 550 nm	MERRA-2	Monthly	0.5^{o} x 0.625^{o}	-
Aerosol (AOD) 550 nm	MODIS-Terra (combined dark target and deep blue)	Daily	1^{o} x 1^{o}	-
Total Angstrom Aerosol Parameter	MERRA-2	Hourly	0.5^{o} x 0.625^{o}	-
Aerosol Single Scattering Albedo (500 nm)	OMI	Daily	1^{o} x 1^{o}	-

2.3.1 Aerosol Parameters

Three aerosol parameters – Aerosol Optical Depth (AOD), Angstrom Exponent (AE) and Single Scattering Albedo (SSA) - were analyzed to investigate the impact of the periods of restrictions and lock-downs during the COVID-19 pandemic on the loading, size distribution and absorption of prevailing atmospheric aerosol over West Africa. See Table 2 for details of the aerosol parameters included in these analyses.

2.3.1.1 Aerosol Optical depth (AOD)

Aerosol optical depth (AOD) is a measure of the extinction of incoming solar radiation by atmospheric aerosol. It quantifies the fraction of light prevented from reaching the Earth's surface by atmospheric aerosols. AOD is one of fundamental optical parameters and a key parameter for the evaluation of aerosol content in atmosphere and air pollution level. While an AOD value of 0.1 indicates a clean atmosphere, a value > 0.5 indicates a hazy and aerosol laden atmosphere. AOD data at 550 nm from both MERRA-2 reanalysis and MODIS-Terra (combined dark target and deep blue) were used to assess the variation in aerosol loading.

MERRA data are managed by NASA's Global Modeling and Assimilation Office (GMAO). GMAO aimed to place historical observations from NASA's Earth Observing System satellites into the Goddard Earth Observing System (GEOS) atmospheric modeling and data assimilation system (Rienecker et al., 2011). MERRA-2, the 2nd version of MERRA, is the latest generation of the reanalysis, which addresses the limitations of the 1st version with the updated Earth system model of GEOS, version 5 (GEOS-5). MERRA-2 is the first long-term global reanalysis to assimilate space-based observations of aerosols and represent their interactions with other physical processes in the climate system.

Although the analyses of the variability of AOD over the sub-region and epicenters were done with MERRA-2 reanalysis AOD parameter, MODIS AOD was used to validate MERRA-2

AOD. MODIS AOD (550 nm) obtained from Moderate Resolution Imaging Spectro-radiometer (MODIS) (Terra) Collection 6.1 aerosol products with the use of combined Dark Target and Deep Blue algorithm was used for the validation. Spatial resolution of radiometer at this wavelength is 1^{o} x 1° for investigation of large areas and with spatial resolution 3 km for investigation aerosols within urban agglomerations.

2.3.1.2 Single Scattering Albedo (SSA)

Single scattering albedo (SSA) relates the ratio of scattering to the extinction coefficient. It depends on particles compositions and volume size distribution in the atmosphere. Although, it is an aerosols optical parameter that is more significant in determining the aerosol radiative effect, SSA is also an important parameter in air quality studies. As the size distribution and composition of the aerosol cluster play significant roles in the determination of SSA values, SSA values can be used to infer the nature, type and sources of the aerosol particles. The values of SSA range from 0 for a purely absorbing aerosol to 1 for a purely scattering aerosol. And, the major absorbing aerosol species are black carbon (BC) (Bond et al., 2013), mineral dust (Claquin et al., 1999) and organic aerosols such as brown carbon (BrC) (Andreae and Gelencsér, 2006).

SSA retrieved by the near-UV two-channel algorithm (OMAERUV) applied to the Aura/Ozone Monitoring Instrument (OMI) measurements was analyzed to assess the impact of restrictions occasioned by the pandemic on optical properties of atmospheric aerosols. SSA data were obtained as time series, area-averaged at wavelength 500 nm, level 3, version 3 data with 1^{o} x 1^{o} spatial resolution (OMAERUVd) from similar satellite OMI but at daily scales and then averaged into monthly mean. Complete SSA data are available for only three of the seven epicenters. As such, the analyses of the SSA data were carried out over the West African sub-region alone. The anomalies in SSA between 2017-2019 and 2020 were computed to assess the

changes in absorption properties of aerosol due to restrictions during the COVID-19 pandemic. Understanding the optical property on dominant aerosol clusters is of great importance as these properties determine their interaction with incoming shortwave and outgoing longwave radiation.

2.3.1.3 Angstrom Exponent (AE)

Angstrom exponent (AE) is an operationally robust optical parameter that contains information on the size distribution of all optically active aerosols in the field of view of a sunphotometer (O'Neill et al., 2001). Analysis of the AE over the epicenters is important as the characterization of the particle sizes distribution will enhance the drawing of inferences about the impact of restrictions due to the COVID-19 pandemic on dominant aerosol particles in the atmosphere in 2020. 30-minute averages of AE are clustered into bins based on the aerosols modes. One constant value of AE is not a good threshold to classify the aerosol types. However, $AE \leq 1.0$ and $AE > 1.0$ is typically representative of coarse-mode and fine-mode dominated aerosols cluster (Kaufman, 1993). The closer the value of AE is to zero, the coarser the aerosol particle.

2.3.2 Gaseous air pollutant

Anthropogenic pollution is estimated using the atmospheric loading of NO_2, CO, SO_2 and O_3 averaged over the region and on a finer scale, the epicenters. Details of the sources, units and spatial resolution of the data are given in Table 2. OMI is an ultraviolet/visible (UV/VIS) nadir solar backscatter spectrometer which makes daily measurement of Earth radiance and solar irradiance from 270 to 500 nm with spectral resolution of 0.5 nm. It provides nearly global coverage in one day, with a spatial resolution of 13 km x 24 km. Atmospheric gases measured are O_3, NO_2, SO_2, HCHO, BrO, and OClO. In addition OMI measures aerosol characteristics, cloud top heights and cloud coverage (Jethva et al., 2014; Levelt et al., 2006). With its high spatial resolution and daily global coverage, OMI promises highly interesting scientific results

that could enhance our understanding of stratospheric and tropospheric chemistry and climate change (Balis et al., 2007).

2.3.2.1 Nitrogen dioxide (NO_2)

NO_2 is an important chemical species in both the stratosphere where it plays a key role in ozone chemistry and in the troposphere where it is a precursor to ozone production. NO_2 is an anthropogenic pollutant emitted from combustion processes, traffic and industrial activities. We use level-3 daily global gridded (0.25^o x 0.25^o) nitrogen dioxide product (OMNO2d). OMNO2d is produced for all atmospheric conditions in the total column NO_2 and the total tropospheric column NO_2, and for sky conditions where cloud fraction is < 30 % (Lamsal et al., 2021).

2.3.2.2 Ozone (O_3)

Ozone is a secondary pollutant as such its atmospheric concentration rely on prevailing meteorology and concentration of its precursors - NO_X ($NO + NO_2$), volatile organic compounds (VOCs) and CO. Majority of tropospheric ozone is formed when NO_X, VOCs and CO react in the presence of sunlight. The prominent sources of these precursors are biomass burning, traffic emission, industrial activities, lightening NO_X and stratospheric injection (Levelt et al., 2006). Two satellite data products are available for total column ozone – TOMS and DOAS. OMI total column ozone data are retrieved using both the TOMS V8 retrieval algorithm developed by NASA (Balis et al., 2007) and a differential optical absorption spectroscopy (DOAS) technique developed by Royal Netherlands Meteorological Institute (KNMI) (Veefkind et al., 2006). Both algorithms provide OMI ozone data of the same quality as TOMS ozone data in order to ensure continuity of ozone trends detected to date. Comparing total ozone products from TOMS V7 retrieval with thirty ground-based station, (McPeters and Labow, 1996) found that the TOMS ozone data compares within ±1% of ground-based measurements.

2.3.2.3 Carbon monoxide (CO)

The atmospheric sources of CO, an odourless, tasteless and colourless, are combustion of fossil fuel, biomass burning and oxidation of methane and biogenic hydrocarbons (Holloway et al., 2000). Monthly mean column burden of CO from MERRA-2 was used to assess the atmospheric levels of CO in this study. MERRA project focuses on historical climate analyses for both weather and climate time scales. This reanalysis covers the period from 1980 to present, continuing as an ongoing climate analysis as resources allow. Several studies, (for example, Cao et al. (2021); Shikwambana (2019); Shikwambana and Kganyago (2021)), have used MERRA2 products such SO_2, BC and CO to investigate the atmospheric concentrations of pollutants both on local and regional scales.

2.3.2.4 Sulphur dioxide (SO_2)

SO_2 is the predominant anthropogenic sulphur-containing air pollutant emitted from the combustion of fossil fuels, which generates mainly SO_2 together with some fraction of other sulphur compounds like SO_3, H_2SO_4 and H_2S. The amount of SO_2 emitted from the combustion of a fossil fuel type depends of the sulphur content of the fuel. Mixing ratios in continental background air range from 20 ppt to 1 ppb. The lifetime of SO_2 is around 1 week on average (Seinfeld and Pandis, 2016).

Hourly averaged SO_2 surface mass concentration (M2T1NXAERV5.12.4) data was used in the analyses undertaken in this study. These were averaged to monthly values to estimate the monthly anomaly of SO_2 over the sub-region and the seven epicenters.

2.4 Statistical analyses

2.4.1 Anomalies

The monthly anomalies of the parameters are computed as the difference between the monthly values for year 2020 and monthly average of the reference years (2017-2019). The mean annual anomaly is taken as the mean of the monthly anomalies. Percentage monthly anomaly is calculated as:

$$Monthly\ anomaly\ (\%) = \left(\frac{monthly\ values\ for\ 2020 - average\ monthly\ values\ of\ ref.\ years}{monthly\ value\ for\ 2020}\right) \times 100 \ldots\ldots (1)$$

2.4.2 Binning of Angstrom Exponent

To examine and classify the size distribution of atmospheric aerosol in the year 2020 in relation to the reference years, bins of the 30 minutes averages of Angstrom Exponent, $AE_{470\text{-}870}$, were created. The binning was created for 2020 and the average of the reference years. For each datasets, thirty (30) bins were created for $AE_{470\text{-}870}$ between 0 and 2.

2.4.3 Correlation, mean bias error and standard deviation

Apart from anomaly, other statistical indicators used in these analyses are defined as:

$$r = \frac{\sum_{i=1}^{n}(x_i-\bar{x})(y_i-\bar{y})}{\sqrt{\left(\sum_{i=1}^{n}(x_i-\bar{x})^2\right)\left(\sum_{i=1}^{n}(y_i-\bar{y})^2\right)}} \quad (2)$$

$$SD = \sqrt{\frac{\sum(x-\bar{x})^2}{n-1}} \quad (3)$$

$$MBE = \frac{1}{n}\sum_{i=1}^{n}(x_i - y_i) \quad (4)$$

where r is the correlation coefficient, SD is the standard deviation, MBE is the mean bias error, n is the number of terms, x and y are the two pairs of data and, $\bar{x}$ and $\bar{y}$ are the mean of x and y.

3 Results and discussion

The comparison of the various pollutants in 2020 relative to the average of reference years was done at both the regional (West Africa) and epicenters levels. The impact of the lockdowns and restrictions on the atmospheric concentration of each pollutant at both local and regional levels was subsequently discussed because the restrictions were more effective in some epicenters than others.

3.1 Aerosol Parameters

3.1.1 AOD

Due to paucity of ground-based measurement, MODIS AOD data was used to validate and assess the representativeness, relative consistency and accuracy of the MERRA2 AOD parameter used in this study. Area averaged daily values of combined dark target and deep blue AOD (550 nm) for land and sea are used for the validation. MERRA2 AOD parameters are used for the intended analyses in this study because MODIS aerosol parameter is not available for Center Region (Cameroun), one of the seven epicenters included in this study.

Table 3 gives the statistical description of the comparison of the two AOD datasets over the West Africa region and at the epicenters. Monthly average AOD for the four years, 2017 - 2020, considered in this study are included in the statistical analyses. The comparison of AOD (550 nm) from MODIS Terra and MERRA-2, shows high correlation (r) levels ($0.76 \leq r \leq 0.98$) of the two datasets at the epicenters and the over the sub-region. The biases in the two datasets in all the epicenters but one and over the sub-region fall within the range of expected bias set by MODIS over the land ($0.05 \pm 0.15 \times$ AOD). The mean bias error (MBE) and absolute bias are calculated to assess and quantify the difference between the two datasets. The two parameters which are from two different sources with very different methodologies give datasets which are highly comparable. AOD estimation by MODIS is slightly higher than that from MERRA2

reanalysis across all the epicenters and over the region except at Bamako. However, the two data are highly correlated across the epicenters and over the region. As such, MERRA2 AOD dataset used for in these analyses is a good representation of the aerosol loading in the study sites.

Table 3: Statistical analyses of the comparison of MODIS and MERRA2 AOD product

Location	r	MBE	Abs. Bias (%)
Abidjan	0.94	0.093	21.2
Accra & Ashanti Region	0.91	0.002	2.7
Bamako	0.76	-0.025	28.0
Centre region	-	-	
Kadiogo	0.87	0.019	3.5
Lagos	0.96	0.090	18.0
Touba	0.98	0.038	14.1
Regional (West Africa)	0.91	0.063	13.2

3.1.1.1 Regional AOD Anomaly

Figure 2 shows the spatial and temporal variation of the anomalies over the West Africa sub-region. The spatial plot in Figure 2(a), the annual average of the anomaly over the region, shows a contrasting distribution of the anomalies over the sub-region. The monthly variation of the anomaly presented in Figure 2(b) shows a decrease of 10 - 18% in aerosol loading (AOD) during the periods of lockdown and restrictions indicated by the red boxes in Figure 2(b). These two boxes indicate the first and second waves of the pandemic in the region. The average annual anomaly of AOD in the region is -5.9 ± 17.1%. This implies that, relative to the reference years, there was a significant reduction in aerosol loading in the year 2020, especially during the lockdown periods which could be attributed to reduced anthropogenic activities in 2020. In Section 3.1.1.2, the anomalies in AOD will be examined at a high resolution over the epicenters.

3.1.1.2 AOD anomalies over epicenters

As presented in Table 1, there are overlaps in the period of restrictions and lockdowns across the epicenters. The effective and level of compliance with the restrictions vary from one epicenter to the other. As such, varying degrees of impacts on the atmospheric aerosol loadings were quantified over the epicenters. Across the seven epicenters, there were significant reductions in aerosol loading (AOD) with the most and least annual mean percentage AOD anomaly of -13.7 ± 30.3% and -0.5 ± 24.9% over Bamako and Abidjan, respectively. The percentage annual mean (±SD) anomalies in AOD over Lagos, Touba, Ashanti region, Kadiogo and Centre region are -2.9 ± 21.1%, -4.8 ± 11.8%, -3.1 ± 28.7%, -4.6 ± 30.4% and -7.3 ± 15.9%, respectively. Figure 3 presents the temporal (monthly) variation of the percentage anomalies in AOD at the seven (7) epicenters.

3.1.2 Angstrom exponent

The binning of 30-minute averages of $AE_{470\text{-}870}$, an aerosol parameter to infer the size distribution of aerosols in a cluster, in the year 2020 and average for the reference years over the seven epicenters is presented in Figure 4. Considering the count of the coarsest particle cluster ($AE_{470\text{-}870} < 0.6$), a comparison of the two sets of data was carried out. Although at varying degree, there were more days of coarse particle dominated aerosol clusters over the epicenters. This is attributable to significantly reduced human activities during the period of restrictions and lockdown. As presented in Figure 4(a) - (g), the total count in the red boxes representing the coarsest particle cluster are more in year 2020 compared to the average of the reference years. Table 4 presents a quantitative description of the statistics of the counts and anomalies in the bins of the coarsest aerosol cluster ($AE \leq 0.6$) shown in Figure 4. These analyses show that there were more coarse particles in the atmosphere in year 2020 than in the reference years which could

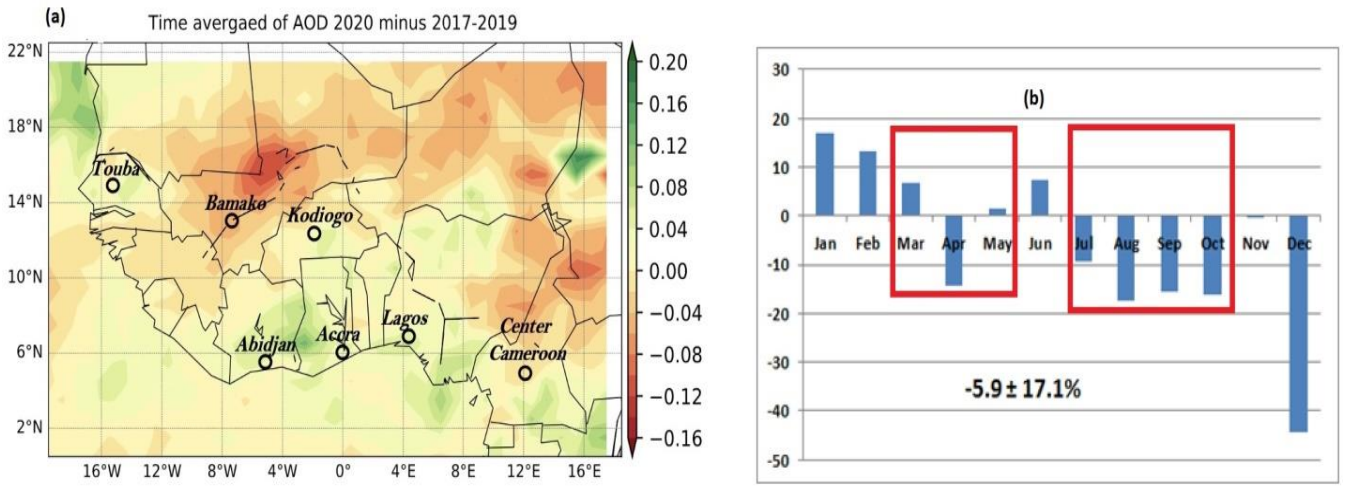

Figure 2: Variation of AOD anomaly over the West Africa sub-region (a) Spatial variation; (b) Temporal (monthly) variation. The red boxes show the period of restrictions across the sub-region.

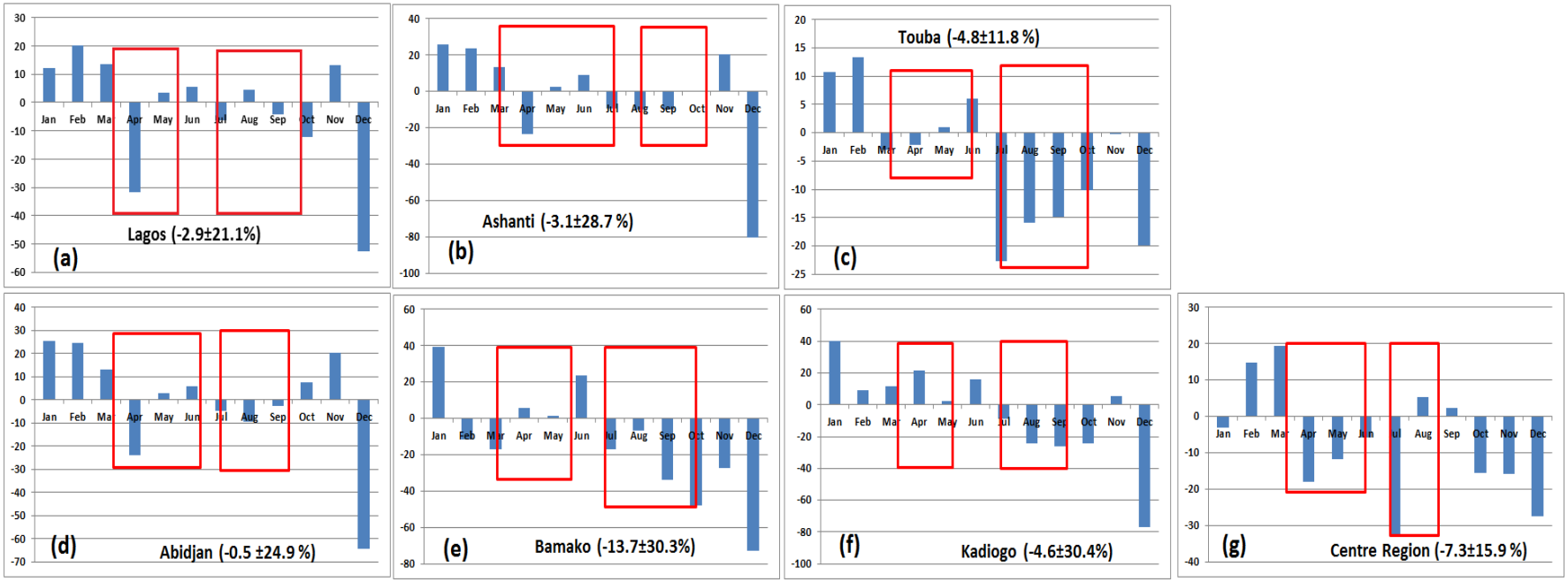

Figure 3: Temporal variation of percentage monthly anomalies of AOD over the epicenters.

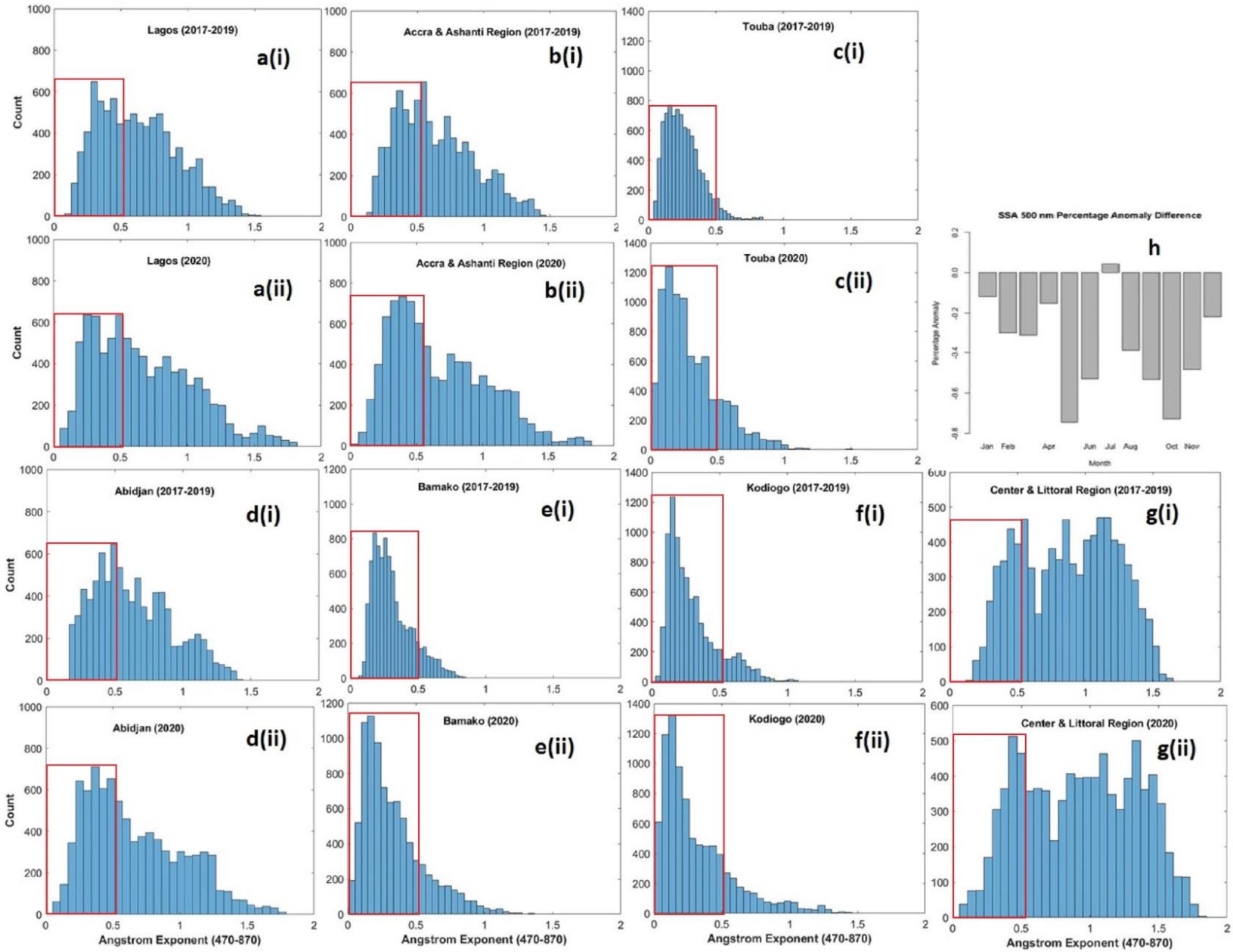

Figure 4: (a-g) Histogram of the binned AE at the epicenters with the red boxes showing the coarsest aerosol bins; (h) monthly anomaly of SSA over West Africa.

invariably impact the nature of interaction between aerosol and incoming shortwave radiation, thereby affecting the Earth's energy budget.

Across all the epicenters except Kadiogo (Burkina Faso), percentage anomaly in Angstrom Exponent (AE ≤ 0.6) ranges between 3 and 28% (see Table 4) indicating a dominance of coarse aerosol particles in the atmosphere in 2020 compared to the reference years.

3.1.3 Single scattering albedo

The monthly anomaly of single scattering albedo (SSA) (500 nm) was computed to quantify the variation in the absorption properties of dominant aerosol cluster in year 2020 relative to the reference years over the sub-region. SSA is an aerosol optical property that could be impacted to a large extent by the size distribution, nature and source of the aerosols.

Table 4: **Statistics of the AE count in the bins and percentage anomaly.**

	AE Bins	**0 - 0.1**	**0.1 - 0.2**	**0.2 - 0.3**	**0.3 - 0.4**	**0.4 - 0.5**	**0.5 - 0.6**	
Abidjan	2017-19	0	6	1006	857	1073	1181	
	2020	0	207	987	1305	607	1200	
	Anomaly (%)		97.1	-1.9	34.3	-76.8	1.6	**10.9**
Lagos	2017-19	0	171	718	1203	1077	907	
	2020	0	258	1143	1079	1156	995	
	Anomaly (%)		33.7	37.2	-11.5	6.8	8.8	**15.0**
Accra	2017-19	0	22	534	1477	971	1221	
	2020	8	294	399	1348	1444	1090	
		100	92.5	-33.8	-9.6	32.8	-12.0	**28.3**
Bamako	2017-19	14	2025	2951	1377	873	682	
	2020	229	2734	1694	1275	954	810	
		93.9	25.9	-74.2	-8.0	8.5	15.8	**10.3**
Centre Region	2017-19	0	3	161	561	782	861	
	2020	0	114	247	306	876	821	
			97.4	34.8	-83.3	10.7	-4.9	**10.9**

Kadiogo	2017-19	406	2225	2423	1513	779	517	
	2020	664	2514	1740	957	458	899	
		38.9	11.5	-39.3	-58.1	-70.1	42.5	**-12.4**
Touba	2017-19	539	2144	2763	1977	896	283	
	2020	606	3379	2076	1213	965	670	
		11.1	36.5	-33.1	-63.0	7.2	57.8	**2.7**

The percentage anomalies in SSA are negative in all the month except July and lie between -0.1 and -0.8 % (see Figure 4(h)). A small anomaly in SSA could cause significant change in aerosol direct radiative forcing depend on the amount and position of cloud cover (above or below aerosol) and surface albedo (Choi and Chung, 2014; Chung, 2012). The slightly enhanced absorbing tendency of dominant aerosol clusters in 2020 compared to the reference years could be attributed to the dominance of coarse particles in the atmosphere in 2020.

3.2 Gaseous pollutants

Atmospheric concentrations of four gaseous pollutants were assessed for 2020 against the reference years (2017-2019). See section 2.3.2 for details and sources of the gaseous pollutants included in the analyses.

3.2.1 Nitrogen dioxide (NO_2)

3.2.1.1 Anomalies in NO_2 levels over the sub-region

As presented in the spatial plot in Figure 5(a), there was significant reduction in the level of atmospheric nitrogen dioxide over the sub-region. Area averaged mean annual anomaly shown in the Figure 4(a) is between 0.5×10^{14} and 3×10^{14} cm^{-2} and the mean (±SD) percentage annual anomaly is -6 ± 4.8 %. The monthly averaged anomalies in NO_2 levels are negative from January through September which coincides with the periods of several restrictions and

lockdown in the sub-region (see Table 1). The monthly anomalies during the 9-month period lie between 2 and 11% (Figure 5(b)). With road traffic and other fossil fuel combustion processes being the primary source of atmospheric NO_2, this significant reduction could be attributed to drastic reduction or total stoppage, in some areas, of traffic flow and industrial activities.

3.2.1.2 Anomalies in NO_2 levels over epicenters

The nature and level of anomalies over the epicenters varies from one center to the other which is arguably due to the extent, level and compliance with the restriction and lockdowns. The mean annual anomaly is negative in four of the seven epicenters and ranges between – 5.7±6.4 % and -14.6±12.8 % (see Figure 6). Although the mean annual anomalies are positive in Ashanti Region, Touba and Abidjan (Figure 6(b), (c) and (d)), there were at least three months with negative anomaly during the period of restrictions in the three epicenters which are indicative of particular times within the several periods of restrictions and lockdowns when there was the most compliance among the populace. In Touba, for instance, the mean anomaly for the four (4) months with negative anomaly is -8.3±5.4% (Figure 6(c)).

3.2.2 Carbon monoxide (CO)

3.2.2.1 Anomalies in CO levels over the sub-region

There is a positive annual mean anomaly (0.9±3.2%) in the level of atmospheric CO over the sub-region in 2020 relative to the reference years. However, as shown in the spatial plot of the anomaly in level of CO over the sub-region (Figure 7), there is a slight decrease in the annual mean anomaly around the coastal countries in the sub-region - Lagos, Abidjan and Accra which could be attributed to a decrease in intrusion of trans-boundary emissions from biomass burning. As presented in Figure 7(b), there are some months with negative anomalies in CO levels in the

atmosphere in 2020 relative to the reference years. These negative anomalies will be observed on a higher resolution over the epicenters in Section 3.2.2.2. Overall, the restrictions and lockdown did not bring about a decrease in CO levels in the cities but rather an increase which could be due increased biomass burning and waste/refuse burning while the restriction lasted.

3.2.2.2 Anomalies in CO levels over epicenters

Annual mean anomalies are positive in all the seven (7) epicenters except Bamako where it is -0.5±4.5%. This implies an increase in annual atmospheric levels in CO in 2020 relative to the reference years. However, just like the case for NO_2 in Ashanti region, Touba and Abidjan, during the months of restrictions and lockdown there were months of negative anomalies in atmospheric CO level in most of the epicenters despite the annual mean anomaly being positive. For instance, in Lagos during March and September while the lockdowns and restrictions lasted, the anomalies were negative except in June and the mean anomaly for these months is -2.0±2.3% (Figure 8(a)). In the other six epicenters, there was at least two months of decrease in atmospheric CO levels except at Kadiogo where the anomaly remained positive all through March to September (see Figure 8(b) – (g)).

3.2.3 Sulphur dioxide (SO_2)

3.2.3.1 Anomalies in SO_2 levels over the sub-region

But for the area around the Sahelian belt, there is significant reduction in the level of atmospheric SO_2 in the sub-region, especially over the cities and urban dwellings (Figure 9(a)). The decrease in atmospheric levels of SO_2 around the cities is similar to the trend observed for NO_2 which is expected as both pollutants are majorly from traffic and industrial processes. As shown in Figure 8(b), the anomalies are negative in March, April, July, August and September,

five of the seven months of extended restrictions and lockdowns in the region. During these five months, the mean anomaly in SO_2 level is -3.5±3.8%.

3.2.3.2 Anomalies in SO_2 levels over epicenters

Across all the epicenters, there is an unequivocal reduction in the levels of atmospheric SO_2. The largest (-10.0±21.5%) and lowest (-3.4±11.9%) reduction are observed in Centre Region and Touba, respectively (see Figure 10). The reduction in SO_2 levels are more pronounced during the second waves of the pandemic in all the seven epicenters. This could be due to the fact that there was more compliance with the restriction and lockdown during the second wave of the pandemic as there were more incidences and fatalities during these periods. The average anomaly over the seven epicenters is -7.0±16.5%. This significant and similar trend in the reduction of SO_2 levels over the cities and dwelling areas is attributable to drastic reduction in traffic movement and industrial activities occasioned by the restrictions because SO_2 is a primary pollutant from the combustion of sulphur-containing fossil fuels.

3.2.4 Ozone (O_3)

Ozone is a secondary pollutant whose level in the atmosphere is significantly impacted by non-linear chemical interactions between volatile organic compounds (VOCs) and NO_X ($NO+NO_2$), a reaction controlled to a large extent by prevailing meso-scale and urban canopy circulation patterns (Marlier et al., 2016; Venter et al., 2020). Ozone titration effect and photochemical ozone formation could significantly affect the level of atmospheric ozone depending on the level of NO_2 and NO available in the atmosphere (Seinfeld and Pandis, 2016).

3.2.4.1 Anomalies in ozone levels over the sub-region

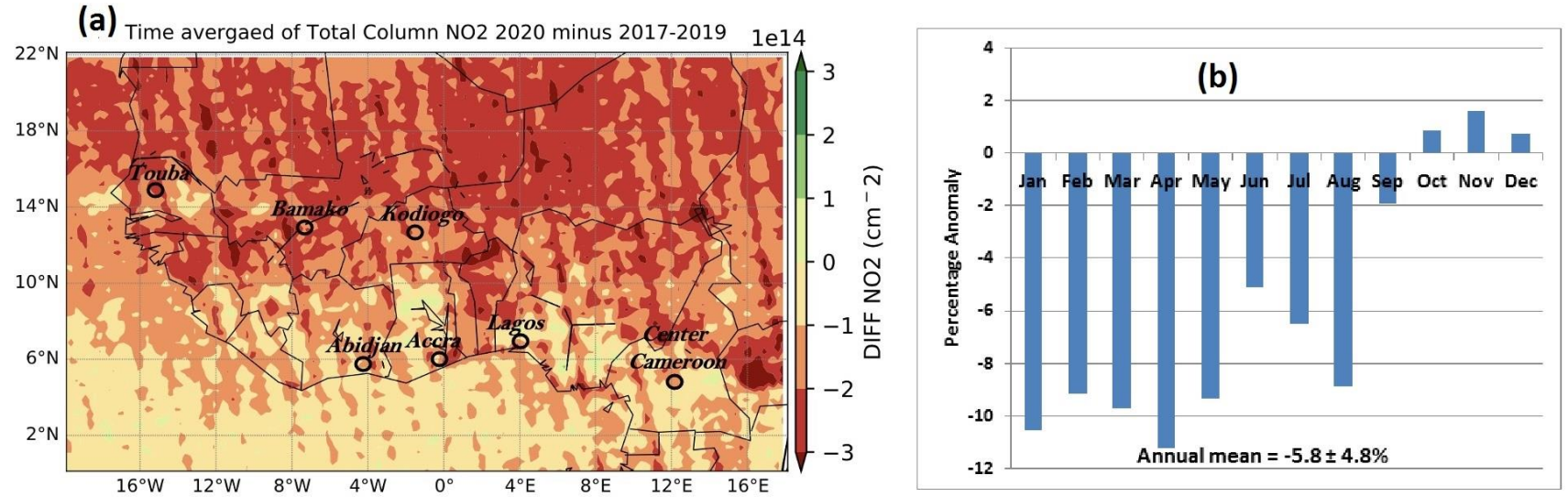

Figure 5: Variation of anomaly in NO_2 levels over the West Africa sub-region (a) Spatial variation; (b) Temporal (monthly) variation.

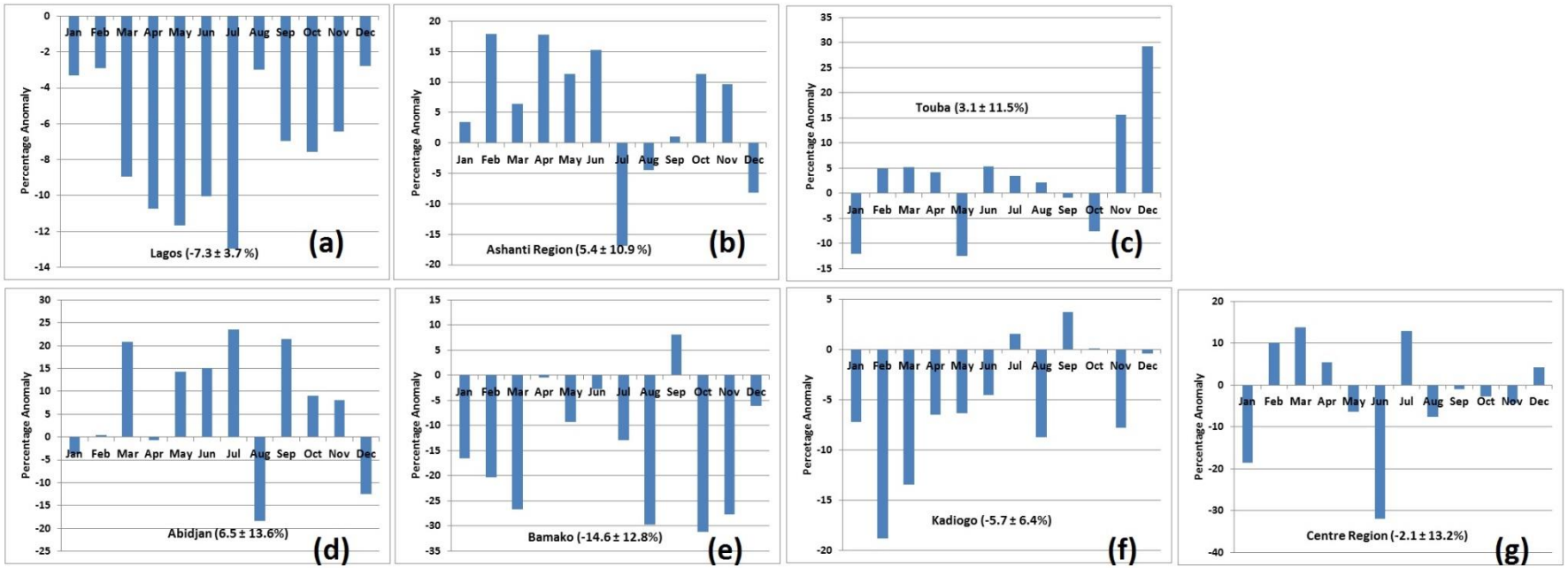

Figure 6: Temporal anomalies of atmospheric NO_2 levels over the epicenters

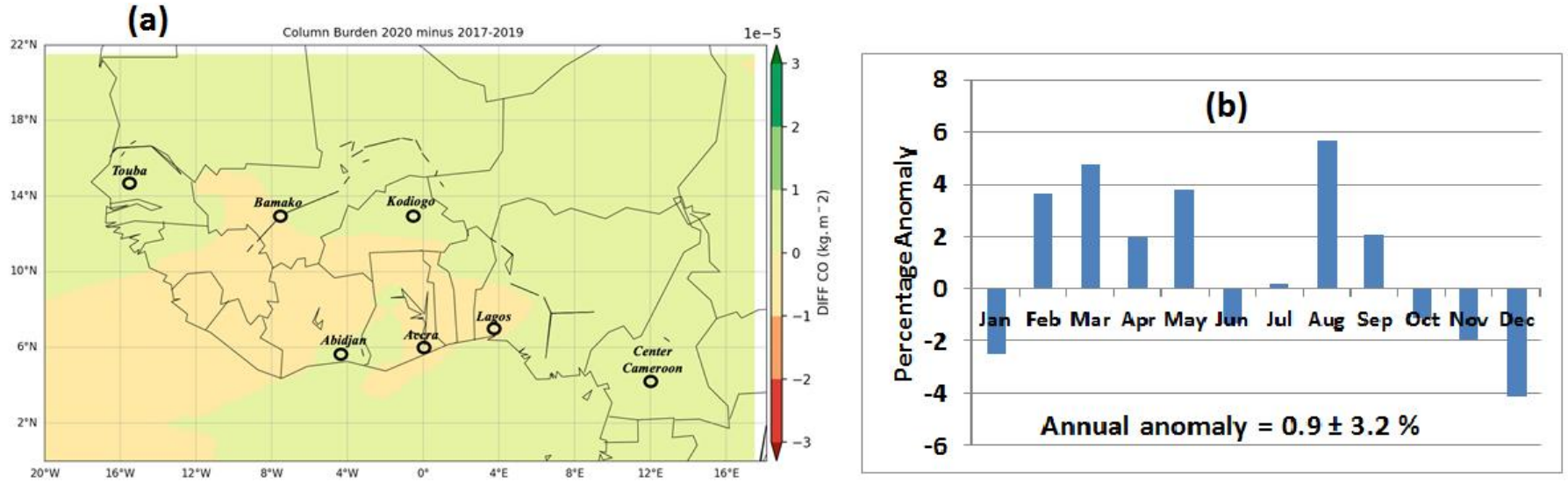

Figure 7: Variation of CO anomaly over the West Africa sub-region (a) Spatial variation; (b) Temporal (monthly) variation.

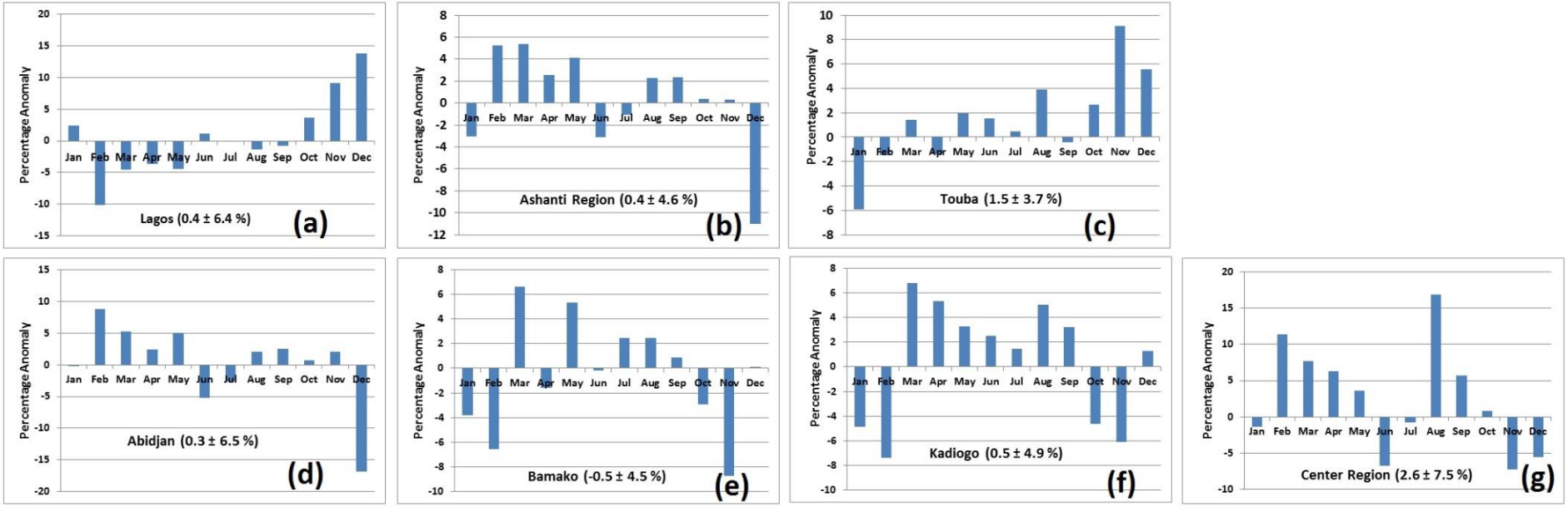

Figure 8: Temporal anomalies of atmospheric CO over the epicenters.

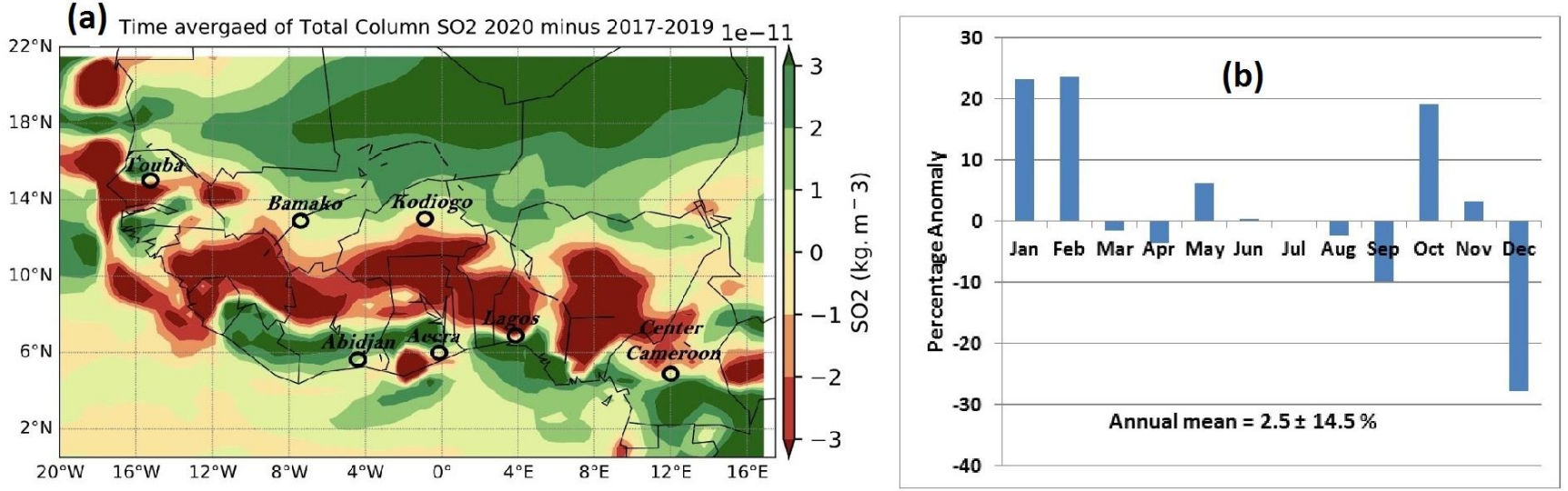

Figure 9: Variation of SO_2 anomaly over the West Africa sub-region (a) Spatial variation; (b) Temporal (monthly) variation.

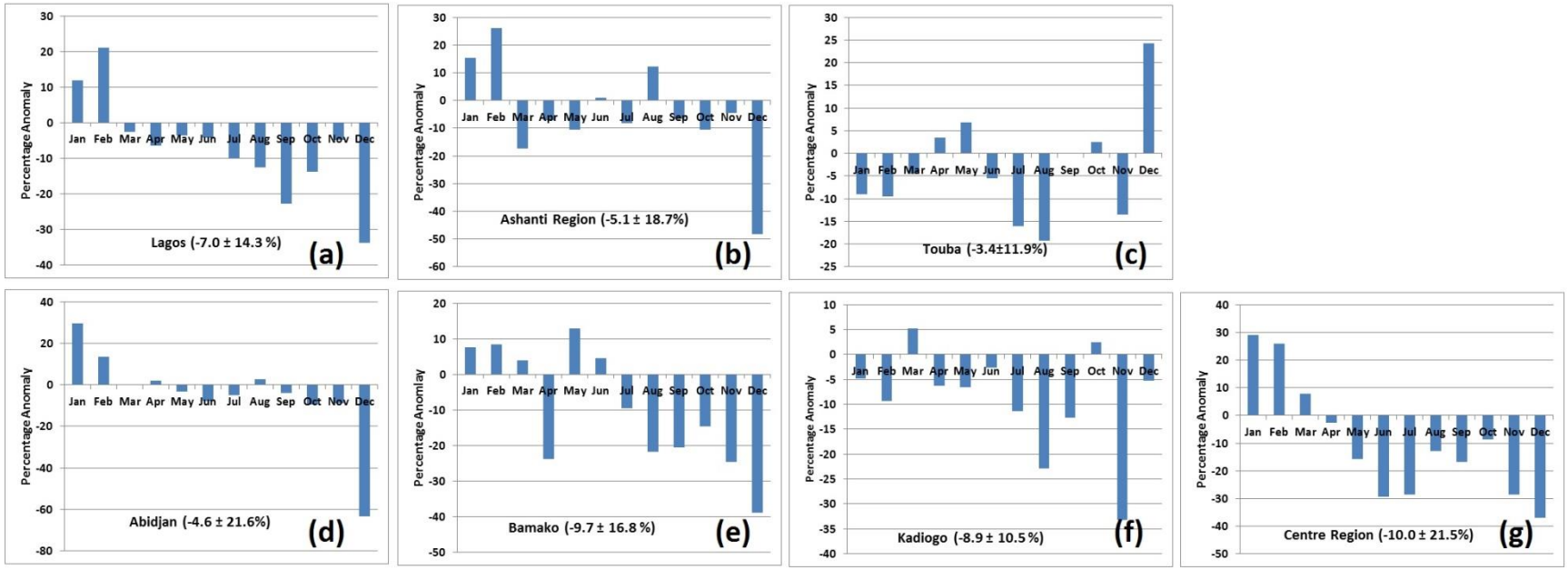

Figure 10: Temporal anomalies of atmospheric SO_2 over the epicenters.

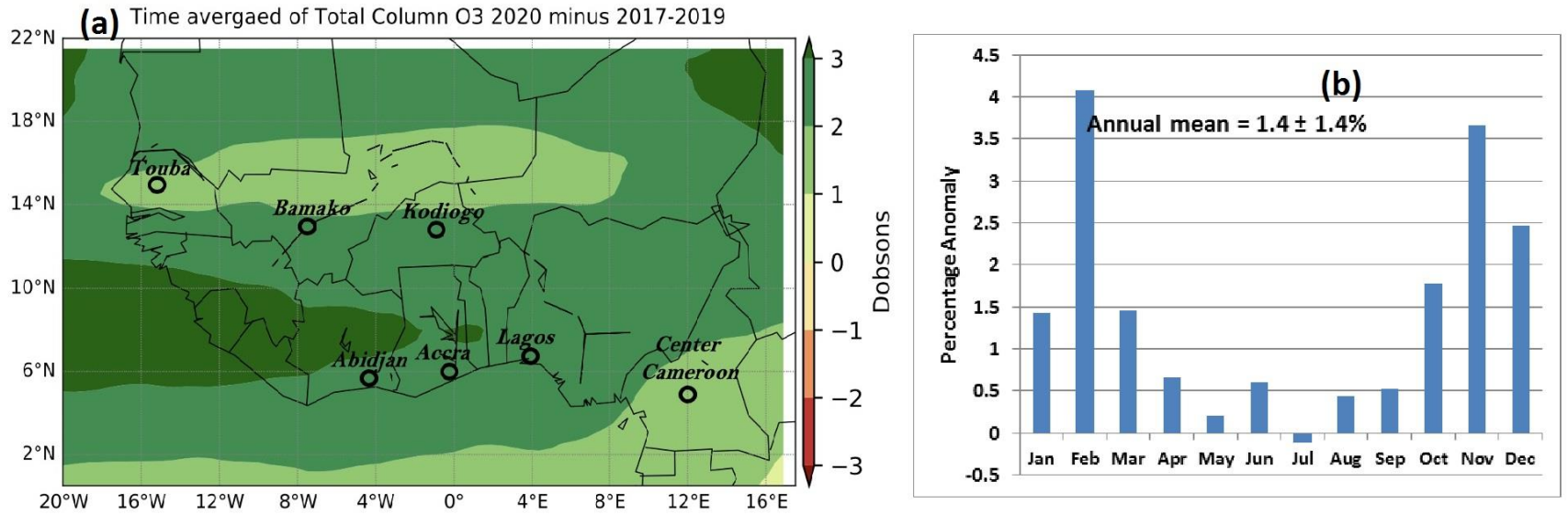

Figure 11: Variation of ozone anomaly over the West Africa sub-region (a) Spatial variation; (b) Temporal (monthly) variation.

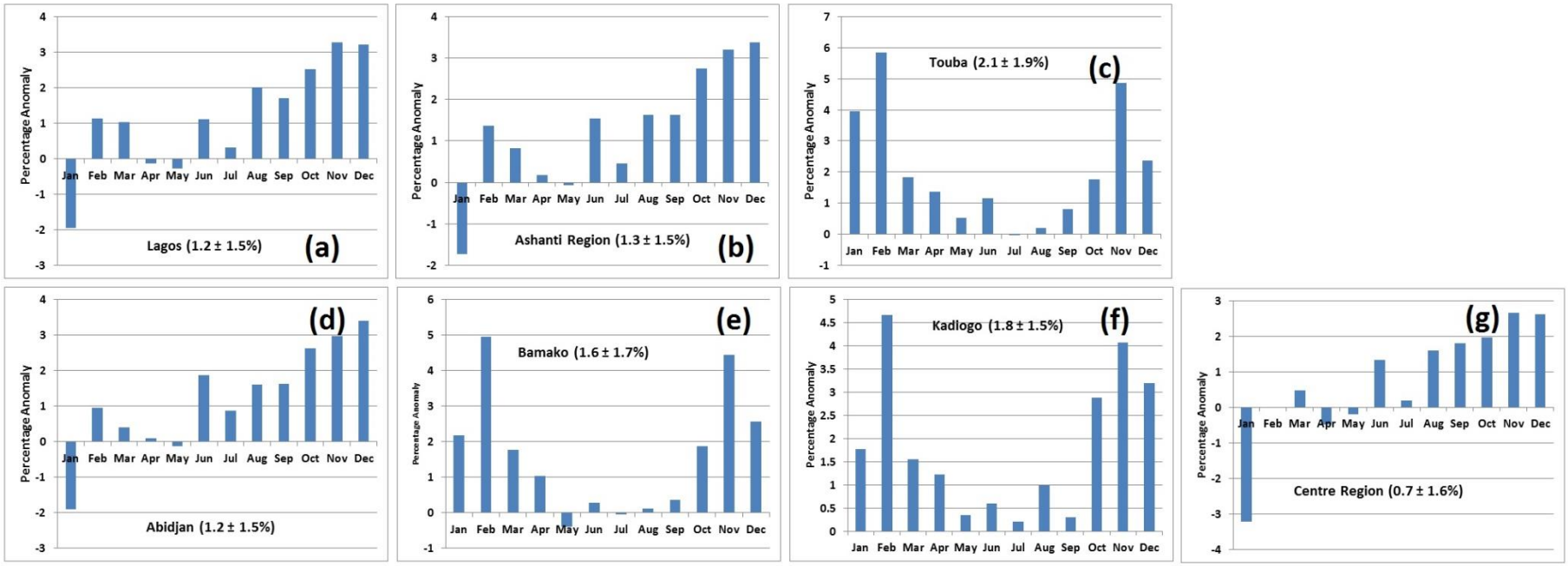

Figure 12: Temporal anomalies of atmospheric ozone over the epicenters.

As shown in Figure 11(a), across the sub-region and over the epicenters, there is a slight increase in the levels of atmospheric ozone. The anomaly in area-averaged ozone levels over the sub-region is 1.4±1.4% and the trend shows a possible impact of prevailing meteorology on the behavior of atmospheric ozone. The bi-modal peak of the anomaly coincides with the onset and peak of the dry season when ambient temperature is always at the highest annually (see Figure 11(b)). The anomaly in ozone level over the sub-region is low during the West African Monsoon, a period characterized by high precipitation and relatively low ambient temperature.

3.2.4.2 Anomalies in ozone levels over epicenters

For most of the months of the year, the anomaly is positive in all the seven epicenters indicating an increase in the levels of atmospheric ozone in 2020 relative to the reference years. The magnitude of increase is more for cities further north of the sub-region, Touba (2.1±1.9%), Kadiogo (1.8±1.5%) and Bamako (1.6±1.7%), as against more coastal cities. The most Southern city, Center Region (Cameroon), has the least anomaly (0.7±1.6%). All of these variations including bi-modal anomaly discussed in section 3.2.4.1 in underpins the impact of prevailing meteorology on the atmospheric concentration of ozone in the sub-region.

Acknowledgement

We want to appreciate NASA for maintaining OMI on Aura's satellite and making available datasets from various platforms on GIOVANNI. We also want to appreciate Global Modeling and Assimilation Office (GMAO) for maintaining and updating MERRA2 AOD dataset. This study has not received any funding.

Data Availability Statement

The data used for the anomalies, temporal analyses (.csv and .xlsx format) and spatial plots of the anomalies (NetCDF) in this study are available at Fawole, Olusegun (2022), "COVID-19: West Africa AQ data", Mendeley Data, V1, doi: 10.17632/3j255ck7yw.1.

Conflict of Interest

The authors declare no conflicts of interest relevant to this study.

4 Conclusions

This aim of the study was to examine the impact of government restrictions on human and vehicular movement during the COVID-19 pandemic in 2020 on the air quality (AQ) in selected epicenters in the West African sub-region as well as over the sub-region. The study resorted to using satellite retrievals and reanalysis due to the non-availability of reliable long-term ground-based AQ data. Finding from the study reveal that there was significant reduction in atmospheric aerosol (AOD), nitrogen dioxide (NO_2) and sulphur dioxide (SO_2) over the sub-region and almost all the epicenters in 2020 compared to the reference years. There was slight increase in the atmospheric levels of carbon monoxide and ozone in the same period. The increase in CO levels could be due to increased biomass burning and waste burning from domestic and communal areas during the lockdown period when people were confined to their local residential areas. The elevated levels of ozone could be due to a number factor including meteorology and atmospheric photochemistry. These suggested that although traffic and industrial activities could be the prominent sources of air pollution in the major cities in the sub-region, there are other sources that could also contribute significantly to AQ problems. As such, policy makers should

realize that a whole and robust AQ management program is needed to improve AQ in urban area significantly.

Although most of the findings from this study are in agreement with those obtained in similar studies carried out across most European and US cities, the elevated level of CO observed over the sub-region and most of the epicenters is a departure from most of these studies. Although ground based measurement would be the best approach to assess these unique local CO levels, knowledge of the local terrain suggests that these elevated level of CO could be from domestic waste burning and biomass burning from agricultural practices.

5 References

Andreae, M.O. and Gelencsér, A., 2006. Black carbon or brown carbon? The nature of light-absorbing carbonaceous aerosols. Atmospheric Chemistry and Physics, 6(10): 3131-3148.

Archer, C.L., Cervone, G., Golbazi, M., Al Fahel, N. and Hultquist, C., 2020. Changes in air quality and human mobility in the USA during the COVID-19 pandemic. Bulletin of Atmospheric Science and Technology, 1(3): 491-514.

Balis, D., Kroon, M., Koukouli, M., Brinksma, E., Labow, G., Veefkind, J. and McPeters, R., 2007. Validation of Ozone Monitoring Instrument total ozone column measurements using Brewer and Dobson spectrophotometer ground-based observations. Journal of Geophysical Research: Atmospheres, 112(D24).

Bauer, S.E., Im, U., Mezuman, K. and Gao, C.Y., 2019. Desert dust, industrialization, and agricultural fires: Health impacts of outdoor air pollution in Africa. Journal of Geophysical Research: Atmospheres, 124(7): 4104-4120.

Bogoch, I.I., Watts, A., Thomas-Bachli, A., Huber, C., Kraemer, M.U. and Khan, K., 2020. Potential for global spread of a novel coronavirus from China. Journal of travel medicine, 27(2): taaa011.

Boiyo, R., Kumar, K.R., Zhao, T. and Bao, Y., 2017. Climatological analysis of aerosol optical properties over East Africa observed from space-borne sensors during 2001–2015. Atmospheric environment, 152: 298-313.

Bond, T.C., Doherty, S.J., Fahey, D., Forster, P., Berntsen, T., DeAngelo, B., Flanner, M., Ghan, S., Kärcher, B. and Koch, D., 2013. Bounding the role of black carbon in the climate system: A scientific assessment. Journal of Geophysical Research: Atmospheres, 118(11): 5380-5552.

Cao, S., Zhang, S., Gao, C., Yan, Y., Bao, J., Su, L., Liu, M., Peng, N. and Liu, M., 2021. A long-term analysis of atmospheric black carbon MERRA-2 concentration over China during 1980–2019. Atmospheric Environment, 264: 118662.

Chen, X. and Yu, B., 2020. First two months of the 2019 Coronavirus Disease (COVID-19) epidemic in China: real-time surveillance and evaluation with a second derivative model. Global health research and policy, 5(1): 1-9.
Choi, J.-O. and Chung, C.E., 2014. Sensitivity of aerosol direct radiative forcing to aerosol vertical profile. Tellus B: Chemical and Physical Meteorology, 66(1): 24376.
Chung, C.E., 2012. Aerosol direct radiative forcing: a review. Atmospheric Aerosols—Regional Characteristics—Chemistry and Physics; Abdul-Razzak, H., Ed: 379-394.
Claquin, T., Schulz, M. and Balkanski, Y., 1999. Modeling the mineralogy of atmospheric dust sources. Journal of Geophysical Research: Atmospheres, 104(D18): 22243-22256.
Diop, D., Kama, A., Drame, M.S., Diallo, M. and Niang, D.N., 2018. The use of ALADIN model and MERRA-2 reanalysis to represent dust seasonal dry deposition from 2006 to 2010 in Senegal, West Africa. Modeling Earth Systems and Environment, 4(2): 815-823.
Dominutti, P., Keita, S., Bahino, J., Colomb, A., Liousse, C., Yoboué, V., Galy-Lacaux, C., Morris, E., Bouvier, L. and Sauvage, S., 2019. Anthropogenic VOCs in Abidjan, southern West Africa: from source quantification to atmospheric impacts. Atmospheric Chemistry and Physics, 19(18): 11721-11741.
Eurosurveillance Editorial Team, 2020. Note from the editors: World Health Organization declares novel coronavirus (2019-nCoV) sixth public health emergency of international concern. Eurosurveillance, 25(5): 200131e.
Fawole, O.G., Cai, X., Levine, J.G., Pinker, R.T. and MacKenzie, A., 2016. Detection of a gas flaring signature in the AERONET optical properties of aerosols at a tropical station in West Africa. Journal of Geophysical Research: Atmospheres, 121(24): 14513–14524.
Fayiga, A.O., Ipinmoroti, M.O. and Chirenje, T., 2018. Environmental pollution in Africa. Environment, development and sustainability, 20(1): 41-73.
Filonchyk, M., Hurynovich, V. and Yan, H., 2021. Impact of Covid-19 lockdown on air quality in the Poland, Eastern Europe. Environmental Research, 198: 110454.
Fu, L., Wang, B., Yuan, T., Chen, X., Ao, Y., Fitzpatrick, T., Li, P., Zhou, Y., Lin, Y.-f. and Duan, Q., 2020. Clinical characteristics of coronavirus disease 2019 (COVID-19) in China: a systematic review and meta-analysis. Journal of Infection, 80(6): 656-665.
Fuwape, I., Okpalaonwuka, C. and Ogunjo, S., 2021. Impact of COVID-19 pandemic lockdown on distribution of inorganic pollutants in selected cities of Nigeria. Air Quality, Atmosphere & Health, 14(2): 149-155.
Hoesly, R.M., Smith, S.J., Feng, L., Klimont, Z., Janssens-Maenhout, G., Pitkanen, T., Seibert, J.J., Vu, L., Andres, R.J. and Bolt, R.M., 2018. Historical (1750–2014) anthropogenic emissions of reactive gases and aerosols from the Community Emissions Data System (CEDS). Geoscientific Model Development, 11(1): 369-408.
Holloway, T., Levy, H. and Kasibhatla, P., 2000. Global distribution of carbon monoxide. Journal of Geophysical Research: Atmospheres, 105(D10): 12123-12147.
Jethva, H., Torres, O. and Ahn, C., 2014. Global assessment of OMI aerosol single-scattering albedo using ground-based AERONET inversion. Journal of Geophysical Research: Atmospheres, 119(14): 9020-9040.
Kaufman, Y.J., 1993. Aerosol optical thickness and atmospheric path radiance. Journal of Geophysical Research: Atmospheres, 98(D2): 2677-2692.
Lamsal, L.N., Krotkov, N.A., Vasilkov, A., Marchenko, S., Qin, W., Yang, E.-S., Fasnacht, Z., Joiner, J., Choi, S. and Haffner, D., 2021. Ozone Monitoring Instrument (OMI) Aura

nitrogen dioxide standard product version 4.0 with improved surface and cloud treatments. Atmospheric Measurement Techniques, 14(1): 455-479.
Lawal, Y., 2021. Africa's low COVID-19 mortality rate: A paradox? International journal of infectious diseases, 102: 118-122.
Levelt, P.F., Hilsenrath, E., Leppelmeier, G.W., van den Oord, G.H., Bhartia, P.K., Tamminen, J., de Haan, J.F. and Veefkind, J.P., 2006. Science objectives of the ozone monitoring instrument. IEEE Transactions on Geoscience and Remote Sensing, 44(5): 1199-1208.
Li, Q., Guan, X., Wu, P., Wang, X., Zhou, L., Tong, Y., Ren, R., Leung, K.S., Lau, E.H. and Wong, J.Y., 2020. Early transmission dynamics in Wuhan, China, of novel coronavirus–infected pneumonia. New England journal of medicine.
Liousse, C., Assamoi, E., Criqui, P., Granier, C. and Rosset, R., 2014. Explosive growth in African combustion emissions from 2005 to 2030. Environmental Research Letters, 9(3): 035003.
Lourens, A.S., Beukes, J.P., Van Zyl, P.G., Pienaar, J.J., Butler, T.M., Beirle, S., Wagner, T.K., Heue, K.-P. and Lawrence, M.G., 2012. Re-evaluating the NO2 hotspot over the South African Highveld. South African Journal of Science, 108(11): 1-6.
Marais, E.A., Jacob, D.J., Kurosu, T., Chance, K., Murphy, J., Reeves, C., Mills, G., Casadio, S., Millet, D. and Barkley, M.P., 2012. Isoprene emissions in Africa inferred from OMI observations of formaldehyde columns. Atmospheric Chemistry and Physics, 12(14): 6219-6235.
Marlier, M.E., Jina, A.S., Kinney, P.L. and DeFries, R.S., 2016. Extreme air pollution in global megacities. Current Climate Change Reports, 2(1): 15-27.
Marticorena, B., Chatenet, B., Rajot, J.-L., Traoré, S., Coulibaly, M., Diallo, A., Koné, I., Maman, A., NDiaye, T. and Zakou, A., 2010. Temporal variability of mineral dust concentrations over West Africa: analyses of a pluriannual monitoring from the AMMA Sahelian Dust Transect. Atmospheric Chemistry and Physics, 10(18): 8899-8915.
Matthias, V., Quante, M., Arndt, J.A., Badeke, R., Fink, L., Petrik, R., Feldner, J., Schwarzkopf, D., Link, E.-M. and Ramacher, M.O., 2021. The role of emission reductions and the meteorological situation for air quality improvements during the COVID-19 lockdown period in central Europe. Atmospheric Chemistry and Physics, 21(18): 13931-13971.
McPeters, R. and Labow, G., 1996. An assessment of the accuracy of 14.5 years of Nimbus 7 TOMS version 7 ozone data by comparison with the Dobson network. Geophysical Research Letters, 23(25): 3695-3698.
Menut, L., Bessagnet, B., Siour, G., Mailler, S., Pennel, R. and Cholakian, A., 2020. Impact of lockdown measures to combat Covid-19 on air quality over western Europe. Science of the Total Environment, 741: 140426.
Naidja, L., Ali-Khodja, H. and Khardi, S., 2018. Sources and levels of particulate matter in North African and Sub-Saharan cities: a literature review. Environmental Science and Pollution Research, 25(13): 12303-12328.
Njenga, M.K., Dawa, J., Nanyingi, M., Gachohi, J., Ngere, I., Letko, M., Otieno, C., Gunn, B.M. and Osoro, E., 2020. Why is there low morbidity and mortality of COVID-19 in Africa? The American journal of tropical medicine and hygiene, 103(2): 564.
Ntoumi, F. and Velavan, T.P., 2021. COVID-19 in Africa: between hope and reality. The Lancet Infectious Diseases, 21(3): 315.
O'Neill, N.T., Dubovik, O. and Eck, T.F., 2001. Modified Ångström exponent for the characterization of submicrometer aerosols. Applied Optics, 40(15): 2368-2375.

Rienecker, M.M., Suarez, M.J., Gelaro, R., Todling, R., Bacmeister, J., Liu, E., Bosilovich, M.G., Schubert, S.D., Takacs, L. and Kim, G.-K., 2011. MERRA: NASA's modern-era retrospective analysis for research and applications. Journal of climate, 24(14): 3624-3648.
Rodriguez-Morales, A.J., Bonilla-Aldana, D.K., Tiwari, R., Sah, R., Rabaan, A.A. and Dhama, K., 2020. COVID-19, an emerging coronavirus infection: current scenario and recent developments-an overview. J Pure Appl Microbiol, 14(1): 5-12.
Schwartz, D.A. and Graham, A.L., 2020. Potential maternal and infant outcomes from coronavirus 2019-nCoV (SARS-CoV-2) infecting pregnant women: lessons from SARS, MERS, and other human coronavirus infections. Viruses, 12(2): 194.
Seinfeld, J.H. and Pandis, S.N., 2016. Atmospheric chemistry and physics: from air pollution to climate change. John Wiley & Sons.
Shikwambana, L., 2019. Long-term observation of global black carbon, organic carbon and smoke using CALIPSO and MERRA-2 data. Remote Sensing Letters, 10(4): 373-380.
Shikwambana, L. and Kganyago, M., 2021. Observations of Emissions and the Influence of Meteorological Conditions during Wildfires: A Case Study in the USA, Brazil, and Australia during the 2018/19 Period. Atmosphere, 12(1): 11.
Spychalski, P., Błażyńska-Spychalska, A. and Kobiela, J., 2020. Estimating case fatality rates of COVID-19. The Lancet. Infectious Diseases.
Srivastava, A.K., Bhoyar, P.D., Kanawade, V.P., Devara, P.C., Thomas, A. and Soni, V.K., 2021. Improved air quality during COVID-19 at an urban megacity over the Indo-Gangetic Basin: From stringent to relaxed lockdown phases. Urban climate, 36: 100791.
Stratoulias, D. and Nuthammachot, N., 2020. Air quality development during the COVID-19 pandemic over a medium-sized urban area in Thailand. Science of the Total Environment, 746: 141320.
Veefkind, J.P., de Haan, J.F., Brinksma, E.J., Kroon, M. and Levelt, P.F., 2006. Total ozone from the Ozone Monitoring Instrument (OMI) using the DOAS technique. IEEE transactions on geoscience and remote sensing, 44(5): 1239-1244.
Venter, Z.S., Aunan, K., Chowdhury, S. and Lelieveld, J., 2020. COVID-19 lockdowns cause global air pollution declines. Proceedings of the National Academy of Sciences, 117(32): 18984-18990.
Veselovskii, I., Goloub, P., Podvin, T., Tanre, D., Silva, A.d., Colarco, P., Castellanos, P., Korenskiy, M., Hu, Q. and Whiteman, D.N., 2018. Characterization of smoke and dust episode over West Africa: comparison of MERRA-2 modeling with multiwavelength Mie–Raman lidar observations. Atmospheric measurement techniques, 11(2): 949-969.
Wadvalla, B.-A., 2020. How Africa has tackled covid-19. bmj, 370.
Yu, Y. and Chen, P., 2020. Coronavirus disease 2019 (COVID-19) in neonates and children from China: a review. Frontiers in pediatrics, 8: 287.
Yusuf, N., Tilmes, S. and Gbobaniyi, E., 2021. Multi-year analysis of aerosol optical properties at various timescales using AERONET data in tropical West Africa. Journal of Aerosol Science, 151: 105625.